CME LIVE OPEN ACCESS

Journal of
Earth & Environmental Waste Management

Review Article

Exploring the Role of Fractional Derivatives on Bioconvection Flow of Casson Fluids in the Solar System

Ahmad Shafique, Muhammad Ramzan* and Mudassar Nazar

Centre for Advanced Studies in Pure and Applied Mathematics, Bahauddin Zakariya University Multan, Pakistan.

Corresponding Author: Muhammad Ramzan, Centre for Advanced Studies in Pure and Applied Mathematics, Bahauddin Zakariya University Multan, Pakistan.

Received: 2024 Jul 26 **Accepted:** 2024 Aug 14 **Published:** 2024 Sep 01

Abstract

The current research explores how entropy generation, heat, and mass transfer impact the motion of a Casson nanofluid when exposed to solar radiation on a vertical plate. This study employs a base fluid composed of polyvinyl alcohol water and considers the presence of copper nanoparticles and gyrotactic microorganisms. Given the increasing utilization of solar plates in various devices, there is a need to develop an effective numerical model for the flow and thermal characteristics of a parabolic trough solar collector (PTSC) mounted on a solar plate. Parabolic trough solar collectors (PTSCs) are solar energy systems that utilize curved mirrors, resembling parabolic troughs, to concentrate sunlight onto a single focal line. This focused sunlight heats the fluid flowing through a plate aligned along the focal line. Based on Fourier›s and Fick›s laws, the governing equations for heat, mass, and momentum have been established, and mathematical modelling is carried out. The Laplace transform method is applied to derive non-dimensional partial differential equations for the energy, mass, and velocity fields. The graphical analysis primarily focuses on the significant impact of key parameters, including the bioconvection Lewis number, magnetic field parameter, Prandtl number, electric field parameter, thermal Grashof number, mass Grashof number, chemical reaction parameter, and Peclet number, related to the flow properties. Increasing the volume fraction and radiation parameter of nanoparticles is shown to enhance the temperature profile. Non-Newtonian nanofluids exhibit great potential for enhancing heat transfer processes and finding diverse applications in solar energy systems, thermal energy systems, and microchip cooling.

Keywords: Casson Nanofluid, Solar Radiations, Gyrotactic Motile Microorganisms, Caputo Derivative

1. Introduction

Solar energy stands out as one of the most crucial forms of renewable energy, boasting minimal environmental impact. This method harnesses clean, inexhaustible energy without the need for any fuel. Natural resources like heat, water, and electricity can be seamlessly integrated with solar energy. Within the realm of solar energy storage, a pressing challenge currently revolves around enhancing the thermal efficiency of solar collectors to meet industrial and technical energy requirements. The performance and operation of solar collectors are significantly affected by issues such as insufficient heat transport and the thermophysical properties of the base fluid. Multiple efforts have been made to improve the thermophysical characteristics of these base fluids. A promising advancement in this field is the emergence of nanofluids, representing the next generation of fluids.

These nanofluids not only exhibit exceptional thermal properties but also unexpected thermal behavior. By incorporating nanoparticles into fluids, we can augment both solar energy storage and heat transfer capabilities.

Ramzan et al., discussed the unsteady and incompressible non-Newtonian fluid flow with fractional derivative. Krishna et al., investigated a transient flow of second-grade fluid between a parallel plate in a porous media [1, 2]. Nazar et al., solved a problem of rate-type fluid through a circular cylinder by the help of Hankel as well as Laplace transforms [3]. Some of the work on non-Newtonian fluids is of Samiulhaq et al., and Sheikh et al [4, 5]. Kataria et al., discussed the soret effect on unsteady MHD flow of chemically and radiating differential-type fluid on a vertical plate [6]. Shah et al., solved the equation of fractional Order Navier Stokes by new semi analytical technique [7]. The fractional derivative is the generalization of the ordinary derivative by taking the non-integer order of differentiation. Due its generalized property the fractional derivative becomes a potent tool to describe the heat and mass transfer phenomena and has attained the attention by researchers. Sene presented the fractionalized model by the Caputo fractional operator on a viscous fluid with Newtonian heating [8]. Razzaque et al., discussed the fractionalized thermal as well as mass transports for differential-type fluid by the the use of Caputo Fabrizio fractional derivative [9]. Chu et al., obtained the analytical solution of the viscous nanofluid model comprehended by a nonlocal constant proportional Caputo (CPC) fractional operator with actual thermophysical properties [10]. Acharya investigated the thermal characteristics of a hybrid nanofluid flowing in a microchannel when sun radiation was present [11]. Song et al., examined the relevance of copper and alumina nanoparticles moving through the water with a rapidly heated surface [12]. Jamshed et al., have addressed the optimization of solar energy utilizing Sutterby hybrid nanofluid in solar HVAC exposed to expanding sheets [13]. Recent studies have looked at the impact of nanoparticles in various fluid types [14-17]. Shahzad et al., study of Oldroyd-B (aluminium alloy-titanium alloy/engine oil) hybrid nanofluid was conducted to examine the thermal cooling effectiveness of a solar water pump [18].

The non-Newtonian behaviour of nanofluids is a topic that scientists and academics are now very interested in. Processes for heat transmission benefit greatly from nanofluid flows. The basic fluids are inefficient in transferring heat. To improve heat transfer efficiency, researchers typically add nanoparticles to the base fluids. These nanoparticles improve the base fluid's conductive qualities. The metals copper, aluminium, silver, titanium, gold, alumina, etc. are common materials for nanoparticles, which are microscopic particles. Nanofluids are base fluids containing a colloidal suspension of nanoparticles.

Nanofluids exhibit enhanced thermal conductivities and diffusivities compared to conventional fluids, positioning them as promising candidates for future heat transfer applications. Their exceptional thermophysical properties have led to their widespread utilization in various fields, including electronics, catalysis, medicine (such as chemotherapy for targeting infected sensorial cells), shipping, pulsating heat pipes, thermosyphons, biomedicine, renewable energy, manufacturing, and transportation. Choudhary and Sharma conducted a study on mixed convectional laminar flows along a vertical surface, examining the effects of mass and heat transfer [19]. Wang et al., explored the unsteady flow of Casson nanofluid using generalized Fourier's and Fick's laws for heat and mass transfer [20]. Bresme and Oettel [21] delved into the movement of nanoparticles at liquid interfaces, while Zokri et al., investigated the impact of suspended nanoparticles on mixed convection Jeffrey flow through a circular horizontal cylinder [22]. Sharma et al., focused on bio-magnetic blood flow within a tapering porosity stenosed artery, considering Soret and Dufour's effects [23]. Naidu et al., examined the effects of partial slip and radiation on Jeffrey nanofluid MHD flow on a vertically extended surface, which also included motile gyrotactic microorganisms [24].

In the realm of chemical engineering, polyvinyl alcohol (PVA), a vital industrial chemical, finds versatile applications. Understanding the flow behavior of PVA solutions and the role of nanoparticles in thermal transfer applications is crucial for executing industrial-scale chemical processes. PVA, although not a natural compound, plays an indispensable role in various sectors, including food production (as a moisture-protective binder and coating agent), release liners, paper coating, fiber manufacturing, and polyvinyl acetate paste production. The incorporation of nanoparticles significantly enhances the thermal and mechanical properties of PVA solutions. Shahzad et al., demonstrated that a copper nanoparticle-infused polyvinyl alcohol-water-based fluid exhibits improved thermal conductivity and heat transfer rates, particularly when subjected to Ohmic heating and viscous dissipation in MHD heat transfer flows of a Cu-PVA Jeffrey nanofluid over a stretchable surface [25]. Giri et al., investigated the flow and heat transfer characteristics of an unstable nanofluid thin film generated by linear stretching velocity across a horizontally placed stretching sheet to achieve better agreement between two sets of data [26]. Hassan et al., explored heat transmission through a wedge and the flow behaviour of a non-Newtonian nanofluid composed of a PVA solution [27].

The phenomenon of a fluid particle suspension's response to a temperature gradient, known as thermophoresis or heat-driven particle motion, has various practical applications such as separating tiny particles, semiconductors, electrostatics, and polymer particles from gas flows. In such suspensions, particles undergo Brownian motion, randomly moving and changing direction upon collision with other particles. This random zigzag motion, which involves the exchange of energy among particles, is known as Brownian diffusion. Heat transfer mechanisms in nanofluids depend on both thermophoresis diffusion and Brownian diffusion. The term "nanofluid" was originally coined by Choi, who highlighted that suspending microscopic nanoparticles in a regular liquid can significantly enhance the liquid's thermal conductivity and heat transfer capabilities [28]. Jang and Choi [29] investigated Brownian motion about the heightened thermal conductivity of nanofluids. Bhattacharya et al., employed Brownian dynamics simulations to compute nanofluid thermal conductivity [30]. Shafique developed a model that considered thermos-diffusion and heat generation effects [31]. Khan and Pop discussed boundary-layer nanofluid flow induced by a linear stretchable surface [32]. The memory impact of velocity and temperature fields is best described by a novel combination proportional Caputo hybrid fractional operator, which Blaenau recently introduced [33]. To investigate the heat transfer flow of clay water-based nanofluids, Imran et al., adopted the (CPC) fractional technique [34]. Saqib et al., examined the (CF) fractional operator on a fractional model of a fluid of the Brinkman type with a hybrid nanostructure [35]. Imran et al., considerations focused on the impact of hybrid nanofluids on the heat transfer motion of a viscous fluid caused by a pressure gradient with a (CPC) fractional derivative [36].

Numerous industrial processes, such as generating electricity, regulating temperatures, chemical reactions, and microelectronics, rely on conventional fluids like ethylene glycol, and heat transfer oil, and water. However, these fluids face limitations in achieving efficient heat transfer due to their comparatively low thermal conductivity. An approach to overcome this limitation involves incorporating extremely small solid nanoparticles into regular fluids to enhance their heat conductivity. Therefore, bioconvection-related studies are carried out with classical models for different geometries, like plate sheets, cylinders, regular and irregular surfaces as discussed in the above literature. There is a gap in the existing literature with the fractional approach of bioconvection. Imran et al., released their study on the fractional bioconvection impact on viscous fluid over a vertical geometry and detailed how to use an integral transform technique to analyze how the fractional parameter and bioconvection number affect the fluid flow [37]. Fourier and Ficks's Laws for Energy and Diffusion Equations were used in their research to develop the Caputo fractional model, and the results were promising. As a result, this study investigates mass concentration, electric and magnetic field, heat generation, thermal radiation, and the effect of solar radiation while taking into account mobile gyrotactic microorganisms and copper nanoparticles in a polyvinyl alcohol-water base fluid using a Caputo fractional operator, which is a linear combination of two fractional operators. The Laplace transform method is used to get analytical solutions, and some graphical results for various flow parameters are provided to illustrate physical behaviour.

1.1. Mathematical Formulation

Consider a xy-coordinate system with an unsteady heat and mass transfer flow of a Casson nanofluid over a flat surface. Concerning surface temperature $T^{\cdot}_{\infty}$ and reference concentration of mass $C^{\cdot}_{\infty}$ and microorganisms and $N^{\cdot}_{\infty}$. respectively, the plate and fluid are initially at rest at time $t = 0$. After some time, the plate starts to move at a steady speed, increasing the plate's concentration of mass and microorganisms $C^{\cdot}_{w}$ and $N^{\cdot}_{w}$, respectively, and surface temperature $T^{\cdot}_{w}$. The following equations may be used to derive the equations of momentum, energy, concentration, and free convection flow of Casson fluid over a vertical plate using the Boussinesq approximation [37]. Momentum equation:

$$\rho_{nf}\frac{\partial u_2(x^{\cdot},t^{\cdot})}{\partial t^{\cdot}} = \mu_{nf}\left(1+\frac{1}{\eta}\right)\frac{\partial^2 u_2(x^{\cdot},t^{\cdot})}{\partial x^{\cdot 2}} - \sigma_{nf}[B_0^2 u_2(x^{\cdot},t^{\cdot}) - HB] +$$

$$g(\rho\beta_{T^{\cdot}})_{nf}(T^{\cdot} - T^{\cdot}_{\infty}) + g(\rho\beta_{C^{\cdot}})_{nf}(C^{\cdot} - C^{\cdot}_{\infty}) - g(\rho\beta_{N^{\cdot}})_{nf}(N^{\cdot} - N^{\cdot}_{\infty}). \quad (1)$$

Energy equation:

$$(\rho C_P)_{nf}\frac{\partial T^{\cdot}(x^{\cdot},t^{\cdot})}{\partial t^{\cdot}} = -[1 + \frac{16\sigma T^{\cdot 3}_{\infty}}{3k_{nf}K^*}]\frac{\partial q_1(x^{\cdot},t^{\cdot})}{\partial x^{\cdot}} + Q_0(T^{\cdot} - T^{\cdot}_{\infty}), \quad (2)$$

the Fourier's law for thermal fluxes

$$q_1(x^{\cdot},t^{\cdot}) = -K_{nf}D_t^{\gamma}\frac{\partial T^{\cdot}(x^{\cdot},t^{\cdot})}{\partial x^{\cdot}}, \quad 1 \geq \gamma > 0. \quad (3)$$

Mass equation:

$$\frac{\partial C^{\cdot}(x^{\cdot},t^{\cdot})}{\partial t^{\cdot}} = -\frac{\partial J_1(x^{\cdot},t^{\cdot})}{\partial x^{\cdot}} - K_1 r_0(C^{\cdot} - C^{\cdot}_0) + \frac{D_T}{T^{\cdot}_{\infty}}\frac{\partial^2 T(x^{\cdot},t^{\cdot})}{\partial x^{\cdot 2}}, \quad (4)$$

the Ficks's law for mass fluxes

$$J_1(x^{\cdot},t^{\cdot}) = -D_m\, D_t^{\gamma}\frac{\partial C^{\cdot}(x^{\cdot},t^{\cdot})}{\partial x^{\cdot}}, \quad 1 \geq \alpha > 0. \quad (5)$$

Bioconvection equation:

$$\frac{\partial N}{\partial t} = -\frac{\partial \omega}{\partial x^{\cdot}} - \frac{bWc}{C^{\cdot} - C^{\cdot}_{\infty}}\frac{\partial}{\partial x^{\cdot}}\left(N\frac{\partial C}{\partial x^{\cdot}}\right) \quad (6)$$

the Ficks's law for bioconvection mass fluxes

$$\omega(x^{\cdot},t^{\cdot}) = -D_n\, D_t^{\gamma}\frac{\partial N}{\partial x^{\cdot}}, \quad 1 \geq \alpha > 0. \quad (7)$$

The physical realistic initial and boundary conditions are

$$u_2(x^{\cdot},0) = 0, \quad T^{\cdot}(x^{\cdot},0) = T^{\cdot}_{\infty}, \quad C^{\cdot}(x^{\cdot},0) = C^{\cdot}_{\infty}, \quad N(x^{\cdot},0) = N_{\infty}, \quad (8)$$

$$u_2(0,t^{\cdot}) = u_0 H(t), \quad T^{\cdot}(0,t) = T_w^{\cdot},$$

$$C^{\cdot}(0,t^{\cdot}) = C_w^{\cdot}, \quad N(0,t^{\cdot}) = N_w, \quad t^{\cdot} > 0, \tag{9}$$

$$u_2(x^{\cdot},t^{\cdot}) \to 0, T^{\cdot}(x^{\cdot},t^{\cdot}) \to T_\infty^{\cdot}, \;\; C^{\cdot}(x^{\cdot},t^{\cdot}) \to C_\infty^{\cdot}, N^{\cdot}(x^{\cdot},t^{\cdot}) \to N_\infty, \;\; x^{\cdot} \to \infty, \quad t^{\cdot} > 0. \tag{10}$$

We have the dimensionless variable

$$y = \frac{U_0 x^{\cdot}}{\nu_f}, \quad t = \frac{t^{\cdot} U_0^2}{\nu_f}, \quad T = \frac{T^{\cdot} - T_\infty^{\cdot}}{T_w^{\cdot} - T_\infty^{\cdot}}, \quad v = \frac{u_2}{U_0}, \quad C = \frac{C^{\cdot} - C_\infty^{\cdot}}{C_w^{\cdot} - C_\infty^{\cdot}}, \quad N = \frac{N - N_\infty}{N_w - N_\infty}, \tag{11}$$

After employing the dimensionless variables, we obtain the following dimensionless governing equations. The dimensionless momentum equation is

$$\frac{\partial v(y,t)}{\partial t} = a_1(A)\frac{\partial^2 v(y,t)}{\partial y^2} + a_2 GrT(y,t) + a_3 GmC(y,t) - a_4 GnN(y,t) - (a_5 Mv(y,t) - H), \tag{12}$$

The dimensionless thermal balance equation given by

$$\frac{\partial T(y,t)}{\partial t} = -\frac{b_1 + Nr}{Pr}\frac{\partial q_1(y,t)}{\partial y} + QT(y,t), \tag{13}$$

the dimensionless Fourier's law for thermal fluxes

$$q_1(y,t) = -D_t^{\gamma}\frac{\partial T(y,t)}{\partial y}, \;\; 1 \geq \gamma > 0. \tag{14}$$

The dimensionless mass balance equation is

$$\frac{\partial C(y,t)}{\partial t} = -\frac{c_1}{L1}\frac{\partial J_1(y,t)}{\partial y} - \frac{1}{L1}\frac{N2}{N1}\frac{\partial^2 T(y,t)}{\partial y^2} - RC(y,t), \tag{15}$$

the dimensionless Ficks's law for mass fluxes

$$J_1(y,t) = -D_t^{\gamma}\frac{\partial C(y,t)}{\partial y}, \;\; 1 \geq \alpha > 0 \tag{16}$$

The dimensionless diffusion balance equation is

$$\frac{\partial N}{\partial t} = -\frac{d_1}{L2}\frac{\partial \omega(y,t)}{\partial y} - \frac{Pe}{L2}\frac{\partial N}{\partial y}\frac{\partial C}{\partial y} - \frac{Pe}{L2}\left(\frac{\partial^2 C}{\partial y^2}\right) \tag{17}$$

The dimensionless bioconvection concentration equation is

$$\omega(x,t) = -\,{}^{C}D_t^{\gamma}\frac{\partial N}{\partial y}, \tag{18}$$

with dimensionless conditions

$$v(,0) = 0, \quad T(y,0) = 0, \quad C(y,0) = 0, \quad N(y,0) = 0, \tag{19}$$

$$v(0,t) = H(t) = 1, \quad T(0,t) = 1, \quad C(0,t) = 1, \quad N(0,t) = 1, \;\; t^{\cdot} > 0, \tag{20}$$

$$v(y,t) \to 0, \quad T(y,t) \to 0, \;\; C(y,t) \to 0, \;\; N(y,t) \to 0, \;\; y \to \infty, \quad t^{\cdot} > 0. \tag{21}$$

Where

$$a_1 = \frac{1}{(1-\phi)^{2.5}[(1-\phi)+\phi\frac{(\rho)_s}{(\rho)_f}]}, \quad a_2 = (1-\phi)+\phi\frac{(\beta_{T^{\cdot}})_s}{(\beta_{T^{\cdot}})_f}, \quad a_3 = (1-\phi)+\phi\frac{(\beta_{C^{\cdot}})_s}{(\beta_{C^{\cdot}})_f},$$

$$a_6 = (1-\phi)+\phi\frac{(\beta_{N^{\cdot}})_s}{(\beta_N)_f}, \quad b_1 = \frac{k_{nf}}{k_f}\frac{1}{[(1-\phi)+\phi\frac{(\rho)_s}{(\rho)_f}]}, \quad c_1 = \frac{(D_m)_{nf}}{D_f}, \quad d_1 = \frac{D_{mnf}}{D_f}, A = \left(1+\frac{1}{\eta}\right),$$

$$Nr = \frac{16\sigma T_{\infty}^{\cdot\,3}}{3k_{nf}K^*}\frac{1}{(1-\phi)+\phi\frac{(\rho C_P)_s}{(\rho C_P)_f}}, \quad Q = \frac{Q_0\nu_f}{u_0^2}\frac{1}{(\rho C_P)_f[(1-\phi)+\phi\frac{(\rho C_P)_s}{(\rho C_P)_f}]}, \quad N2 = \frac{\tau D_T(T_w^{\cdot}-T_{\infty}^{\cdot})}{T_{\infty}^{\cdot}\nu_f}, \quad N1 = \frac{\tau D_B(C_w^{\cdot}-C_{\infty}^{\cdot})}{\nu_f},$$

$$R = \frac{\nu_f}{u_0^2}kr_0, \quad Pr = \frac{(\mu C_P)_f}{k_f}, \quad L1 = \frac{\nu_f}{D_m}, \quad L2 = \frac{\nu_f}{D_n}, \quad Pe = \frac{bW_c}{D_m}, \quad a_5 = 1+\frac{3(\frac{\sigma_s}{\sigma_f}-1)\phi}{(\frac{\sigma_s}{\sigma_f}+2)-(\frac{\sigma_s}{\sigma_f}-1)\phi} \tag{22}$$

1.2. Thermophysical Features of Nanofluid

In this section, thermophysical properties are defined in [29,38] as follows:

$$\rho_{nf} = (1-\phi)\rho_f + \phi\rho_s, \quad \mu_{nf} = \frac{\mu_f}{(1-\phi)^{2.5}}, \quad (\rho C_P)_{nf} = (1-\phi)(\rho C_P)_f + \phi(\rho C_P)_s,$$

$$\frac{k_{nf}}{k_f} = \frac{k_s+2k_f-2\phi(k_f-k_s)}{k_s+2k_f+2\phi(k_f-k_s)}, \quad \frac{\sigma_{nf}}{\sigma_f} = 1+\frac{3(\frac{\sigma_s}{\sigma_f}-1)\phi}{(\frac{\sigma_s}{\sigma_f}+2)-(\frac{\sigma_s}{\sigma_f}-1)\phi}, \quad (\beta_T)_{nf} = (1-\phi)(\beta_T)_f + \phi(\beta_T)_s,$$

$$(\beta_C)_{nf} = (1-\phi)(\beta_C)_f + \phi(\beta_C)_s, \quad (\beta_N)_{nf} = (1-\phi)(\beta_N)_f + \phi(\beta_N)_s,$$

where μ_{nf}, $(\rho C_p)_{nf}$, ρ_{nf}, k_{nf}, σ_{nf}, ϕ, $(\beta_T)n_f$, $(\beta_C)_{nf}$ and $(\beta_N)_{nf}$ are the effective dynamic viscosity, heat capacitance, effective density, effective thermal conductivity, effective electrical conductivity, volume fraction of nanoparticles, thermal expansion coefficient, concentration thermal expansion coefficient, and microorganism thermal expansion coefficient respectively.

Table 1: Thermophysical Properties of Nanofluids.

Material	ρ	k	σ	β×10^{-5}	C_p
Copper	8933	400	5.96 × 10^{7}	1.67	385
PVA	1020	0.2	11.7× 10^{-6}	2.5	2000
Water	997	0.613	0.05	21	4179

1.3. Solution of Problem

Calculation of the Temperature:

Taking Laplace transform on Eqs. (13) and (14), we have

$$s\tilde{T}(y,s) = -\frac{b_1+Nr}{Pr}\frac{d\tilde{q_1}(y,s)}{dy} + Q\tilde{T}(y,s) \tag{23}$$

$$\tilde{q_1}(y,s) = -s^{\gamma}\frac{d\tilde{T}(y,s)}{dy} \tag{24}$$

Substituting Eq. (24) in Eq. (23), we obtain

$$\frac{d^2\tilde{T}}{dy^2} - \frac{Pr(s-Q)}{(b_1+Nr)s^{\gamma}}\tilde{T}(y,s) = 0. \tag{25}$$

Also, apply Laplace transform on Eqs. (19) and (20), we get

$$\tilde{T}(0,s) = \frac{1}{s}, \quad \tilde{T}(y,0) = 0. \tag{26}$$

Using Eq. (26) in Eq. (25), the general solution of temperature profile

$$\tilde{T}(y,s) = \frac{1}{s}\, e^{-y\sqrt{\frac{PrPr\,(s-Q)}{(b_1+Nr)s^{\gamma}}}}. \tag{27}$$

Calculation of Concentration:

Taking Laplace transform on Eqs. (15) and (16), we have

$$s\tilde{C}(y,s) = -\frac{c_1}{L1}\frac{d\tilde{J_1}(y,s)}{dy} + \frac{1}{L1}\frac{N_t}{N_b}\frac{d^2\tilde{T}(y,s)}{dy^2} - R\tilde{C}(y,s) \tag{28}$$

$$\tilde{J_1}(y,s) = -s^{\gamma}\frac{d\tilde{C}(y,s)}{dy} \tag{29}$$

Substituting Eq. (29) in Eq. (28), we obtain

$$\frac{d^2\tilde{C}}{dy^2} - \frac{(s+R)L1}{c_1 s^{\gamma}}\tilde{C}(y,s) = \frac{-1}{c_1 s^{\gamma}}\frac{N2}{N1}\frac{d^2\tilde{T}(y,s)}{dy^2} \tag{30}$$

Also, apply Laplace transform on Eqs. (19) and (20), we get

$$\tilde{C}(0,s) = \frac{1}{s}, \qquad \tilde{C}(y,0) = 0. \tag{31}$$

Using Eq. (31) in Eq. (30), the general solution of the concentration profile becomes

$$\tilde{C}(y,s) = \frac{1}{s}e^{-y\sqrt{\frac{(s+R)L1}{c_1 s^{\gamma}}}}\frac{1}{[\frac{PrPr\,(s-Q)}{(b_1+Nr)s^{\gamma}} - \frac{(s+R)L1}{c_1 s^{\gamma}}]}\frac{N2}{N1}$$

$$\times\frac{Pr(s-Q)}{(b_1+Nr)s^{2\gamma}}\left[\frac{1}{s}e^{-y\sqrt{\frac{(s+R)Le}{c_1 s^{\gamma}}}} - \frac{1}{s}\, e^{-y\sqrt{\frac{Pr(s-Q)}{(b_1+Nr)s^{\gamma}}}}\right] \tag{32}$$

Calculation of Bioconvection:

Taking Laplace transform on Eqs. (17) and (18), we have

$$s\tilde{N}(y,s) = -\frac{d_1}{L2}\frac{d\tilde{\omega}(y,s)}{dy} - \frac{Pe}{L2}\frac{d\tilde{N}(y,s)}{dy}\frac{d\tilde{C}(y,s)}{dy} - \frac{Pe}{L1}\frac{d^2\tilde{C}(y,s)}{dy^2} \tag{33}$$

$$\tilde{\omega}(y,s) = -s^{\gamma}\frac{d\tilde{N}(y,s)}{dy} \tag{34}$$

Substituting Eq. (34) in Eq. (33), we obtain

$$\frac{d^2\tilde{N}}{dy^2} - \{-\frac{Pe}{s}\sqrt{\frac{(s+R)L1}{c_1 s^{\gamma}}}\, e^{-y\sqrt{\frac{(s+R)Le}{c_1 s^{\gamma}}}} + \frac{1}{[\frac{PrPr\,(s-Q)}{(b_1+Nr)s^{\gamma}} - \frac{(s+R)L1}{c_1 s^{\gamma}}]}\times\frac{N2}{N1}[-\frac{1}{s}\sqrt{\frac{(s+R)L1}{c_1 s^{\gamma}}}\, e^{-x\sqrt{\frac{(s+R)Le}{c_1 s^{\gamma}}}} +$$

$$\frac{1-e^{-s}}{s^2}\sqrt{\frac{PrPr\,(s-Q)}{(b_1+Nr)s^{\gamma}}}\, e^{-x\sqrt{\frac{PrPr\,(s-Q)}{(b_1+Nr)s^{\gamma}}}}]\}\frac{d\tilde{N}(y,s)}{dy} - \frac{L2}{d_1}\Big[s + \frac{Pe}{\tilde{N}}[-\frac{1}{s}\Big(\frac{(s+R)L1}{c_1 s^{\gamma}}\Big)e^{-y\sqrt{\frac{(s+R)Le}{c_1 s^{\gamma}}}} +$$

$$\frac{1}{[\frac{PrPr\,(s-Q)}{(b_1+Nr)s^{\gamma}} - \frac{(s+R)L1}{c_1 s^{\gamma}}]}\times\frac{N2}{N1}\frac{PrPr\,(s-Q)}{(b_1+Nr)s^{2\gamma}}\Big(\frac{1}{s}\Big(\frac{(s+R)L1}{c_1 s^{\gamma}}\Big)e^{-y\sqrt{\frac{(s+R)Le}{c_1 s^{\gamma}}}} -$$

$$\frac{1}{s}(\frac{PrPr\,(s-Q)}{(b_1+Nr)s^{\gamma}})e^{-y\sqrt{\frac{Pr(s-Q)}{(b_1+Nr)s^{\gamma}}}}\Big)]\Big]\tilde{N}(y,s) = 0, \tilde{N} \neq 0$$

(35)

$$a\frac{d^2\tilde{N}}{dx^2} - b\frac{d\tilde{N}(x,s)}{dx} - c\tilde{N}(y,s) = 0 \tag{36}$$

Also, apply Laplace transform on Eqs. (19) and (20), we get

$$\tilde{N}(0,s)=\frac{1}{s}, \quad \tilde{N}(y,0)=0. \tag{37}$$

Using Eq. (37) in Eq. (36), the general solution of the concentration profile becomes

$$\tilde{N}(y,s)=\frac{1}{s}e^{-y\sqrt{\frac{(b\pm\sqrt{b^2+4c)}}{2}}} \tag{38}$$

Where

a=1

$$b=\{-\frac{Pe}{s}\sqrt{\frac{(s+R)L1}{c_1 s^\gamma}}\,e^{-x\sqrt{\frac{(s+R)Le}{c_1 s^\gamma}}}+\frac{1}{\left[\frac{PrPr\,(s-Q)}{(b_1+Nr)s^\gamma}-\frac{(s+R)L1}{c_1 s^\gamma}\right]}\times\frac{N2}{N1}\frac{PrPr\,(s-Q)}{(b_1+Nr)s^{2\gamma}}\,[-\frac{1}{s}\sqrt{\frac{(s+R)L1}{c_1 s^\gamma}}\,e^{-x\sqrt{\frac{(s+R)Le}{c_1 s^\gamma}}}+\frac{1}{s}\sqrt{\frac{PrPr\,(s-Q)}{(b_1+Nr)s^\gamma}}\,e^{-x\sqrt{\frac{PrPr\,(s-Q)}{(b_1+Nr)s^\gamma}}}\}$$

$$c=\frac{L2}{d_1}\left[s+\frac{Pe}{\tilde{N}}\,[-\frac{1}{s}\left(\frac{(s+R)L1}{c_1 s^\gamma}\right)e^{-x\sqrt{\frac{(s+R)Le}{c_1 s^\gamma}}}+\frac{1}{\left[\frac{PrPr\,(s-Q)}{(b_1+Nr)s^\gamma}-\frac{(s+R)L1}{c_1 s^\gamma}\right]}\times\frac{N_t}{N_b}\frac{PrPr\,(s-Q)}{(b_1+Nr)[s^\gamma]s^{2\beta}}\left(\frac{1}{s}\left(\frac{(s+R)L1}{c_1 s^\gamma}\right)e^{-x\sqrt{\frac{(s+R)Le}{c_1 s^\gamma}}}-\frac{1}{s}\left(\frac{PrPr\,(s-Q)}{(b_1+Nr)s^\gamma}\right)e^{-x\sqrt{\frac{Pr(s-Q)}{(b_1+Nr)s^\gamma}}}\right)]\right] \tag{39}$$

Calculation of Velocity:

Taking Laplace transform on Eqs. (12), we have

$$\frac{d^2\tilde{u}(y,s)}{dy^2}-\frac{(s+a_5M-H)}{a_1(A)}\tilde{u}(y,s)=-\frac{a_2}{a_1(A)}Gr\tilde{T}(y,s)-\frac{a_3}{a_1(A)}Gm\tilde{C}(y,s)+\frac{a_4}{a_1(A)}Gn\tilde{N}(y,s). \tag{40}$$

Putting the value of $\tilde{T}(y,s)$, $\tilde{C}(y,s)$, and $\tilde{N}(y,s)$ in above equation, we obtain

$$\frac{d^2\tilde{u}(y,s)}{dy^2}-\frac{(s+a_5M-H)}{a_1(A)}\tilde{u}(y,s)=-\frac{a_2}{a_1(A)}Gr\left(\frac{1}{s}\;e^{-y\sqrt{\frac{PrPr\,(s-Q)}{(b_1+Nr)s^\gamma}}}\right)-\frac{a_3}{a_1(A)}Gm(\frac{1}{s}e^{-y\sqrt{\frac{(s+R)L1}{c_1 s^\gamma}}}\frac{1}{\left[\frac{PrPr\,(s-Q)}{(b_1+Nr)s^\gamma}-\frac{(s+R)L1}{c_1 s^\gamma}\right]}\frac{N2}{N1}\times\frac{Pr(s-Q)}{(b_1+Nr)s^{2\gamma}}\left[\frac{1}{s}e^{-y\sqrt{\frac{(s+R)Le}{c_1 s^\gamma}}}-\frac{1}{s}\;e^{-y\sqrt{\frac{Pr(s-Q)}{(b_1+Nr)s^\gamma}}}\right])-\frac{a_4}{a_1(1+\lambda s)}Gn(\frac{1}{s}e^{-y\sqrt{\frac{(b\pm\sqrt{b^2+4c)}}{2}}}). \tag{41}$$

Also, apply Laplace transform on Eqs. (19) and (20), we get

$$\tilde{u}(0,s)=\frac{1}{s}, \quad \tilde{u}(y,0)=0. \tag{42}$$

$$\tilde{u}(y,s)=\frac{1}{s}e^{-y\sqrt{\frac{(s+a_5M-H)}{a_1A}}}+Gr\frac{a_2}{a_1(A)s}\frac{1}{\left[\frac{PrPr\,(s-Q)}{(b_1+Nr)s^\gamma}-\frac{(s+a_5M-H)}{a_1(A)}\right]}-\frac{1}{\left[\frac{PrPr\,(s-Q)}{(b_1+Nr)s^\gamma}-\frac{(s+R)L1}{c_1 s^\gamma}\right]}\frac{N2}{N1}\frac{1}{s}\times$$

$$\frac{PrPr\ (s-Q)}{(b_1+Nr)[(1-as^{-a})^{\gamma}]^2 s^{2\beta}} \frac{\left[\frac{1}{s} e^{-y\sqrt{\frac{(s+a_5M-H)}{a_1\mathrm{A}}}} - \frac{1}{s}\ e^{-y\sqrt{\frac{PrPr\ (s-Q)}{(b_1+Nr)[s^{\gamma}]}}}\right]}{\left[\frac{PrPr\ (s-Q)}{(b_1+Nr)s^{\gamma}} - \frac{(s+a_5M-E)}{a_1(A)}\right]} + Gm \frac{1}{\left[\frac{(s+R)L1}{c_1\left[\frac{k_1(a)}{s}+k_O(a)\right]s^{a}} - \frac{(s+a_5M-H)}{a_1(A)}\right]} \frac{a_3}{a_1(A)} \times \left[\frac{1}{s} + \right.$$

$$\left. \frac{1}{\frac{PrPr\ (s-Q)}{(b_1+Nr)\left[\frac{k_1(a)}{s}+k_O(a)\right]s^{a}} - \frac{(s+R)L1}{c_1\left[\frac{k_1(a)}{s}+k_O(a)\right]s^{a}}} \frac{N2}{N1} \frac{1}{s}\ \frac{PrPr\ (s-Q)}{(b_1+Nr)[(1-as^{-a})^{\gamma}]^2 s^{2\beta}}\right] \times \left[e^{-y\sqrt{\frac{(s+a_5M-H)}{a_1\mathrm{A}}}} - e^{-y\sqrt{\frac{(s+R)L1}{c_1 s^{\gamma}}}}\right] -$$

$$Gn \frac{1}{\left[\frac{\left(b\pm\sqrt{b^2+4c}\right)}{2} - \frac{(s+a_5M-H)}{a_1A)}\right]} \frac{a_4}{a_1(1A)s} \left[e^{-y\sqrt{\frac{(s+a_5M-H)}{a_1\mathrm{A}}}} - e^{-y\sqrt{\frac{\left(b\pm\sqrt{b^2+4c}\right)}{2}}}\right]. \quad (43)$$

Eqs. (27,32,38,43) are more complicated, so these cannot be solved analytically. Numerical result of these equations will be obtained by using algorithm [34,35].

2. Result and Discussion

The relationship between the Grashof number (Gr) and fluid velocity, reveals that as Gr increases, fluid velocity also increases depicted in Figure 1. This is because higher Gr values lead to a more substantial temperature gradient and an augmented buoyancy force, resulting in the acceleration of fluid flow. Figure 2 illustrates the connection between Gm and flow field velocity. The findings indicate that higher Gm values are associated with greater fluid velocity due to an intensified buoyancy force. This force induces a pressure gradient within the flow field, accelerating fluid. Consequently, as Gm values rise, fluid velocity increases as well. In Figure 3, we examine the impact of the velocity profile on the bioconvection Rayleigh number, Gn. Here, we observe that increasing Gn values coincide with a decrease in fluid velocity. This graph demonstrates that higher values of the bioconvection Rayleigh number (Gn) impede the upward movement of nanofluid.

In Figure 4, the impact of electric field strength (H) on fluid velocity is presented, indicating that the fluid velocity increases by increasing the value of electric field strength H. As the electric field strength (E) increases, the nanofluid flow is accelerated, leading to an enhancement in fluid velocity. In Figure 5, the impact of magnetic parameter (M) on the velocity distribution is presented. Due to this Lorentz force occurs that reduces the fluid velocity. Figure 6, demonstrates the influence of the concentration of nanoparticles on the velocity field. The velocity profile decreases as the concentration of nanoparticles increases. This figure portrays the effect of the concentration of ternary nanoparticles on the velocity. The results indicate that higher values of (ϕ) result in a stronger viscous force, causing the boundary layer to become denser and subsequently leading to a decrease in velocity.

Figure 7 illustrates the impact of parameter Pr on the fluid velocity. Figure 8 represents the influences of Sc on fluid velocity. In Figure 9, the influence of Nr (radiation parameter) on the temperature is depicted, demonstrating that an increasing radiation parameter leads to an elevation in the fluid temperature. The thermal radiation contributes thermal energy to the stretching surface, resulting in an enhanced temperature profile of the fluid due to conduction between the surface and the fluid. The impact of Pr on fluid temperature is depicted in Figure 10. Pr represents the ratio of momentum (product of mass and velocity) diffusion to thermal diffusion. For the larger value of Pr, diffusion of heat becomes slow as compared to the fluid momentum (velocity) which decreases the thermal conductivity (thickness) and raises the momentum. Figure 11 illustrates that as N1 increases, the concentration profile experiences an increase in particle accumulation or depletion. Thermophoresis can cause particles to migrate towards regions of higher or lower temperature, depending on the properties of the particles and the fluid. Consequently, an increase in thermophoresis diffusion leads to a more pronounced concentration profile, with higher peaks or deeper troughs, depending on the direction of particle migration. Thus, an increase in thermophoresis diffusion (N1) enhances the effect of temperature gradients on the concentration profile, resulting in more distinct accumulation or depletion regions of particles within the fluid.

Figure 12 illustrates that as N2 increases, the concentration profile experiences a decrease in sharp concentration gradients, leading to a more uniform distribution of particles. This is because Brownian motion causes particles to undergo random movements, resulting in enhanced diffusion and increased collisions between particles. Consequently, the particles spread out more evenly throughout the fluid, leading to a smoother concentration profile. So, an increase in Brownian motion (N2) decreases the concentration profile by promoting better mixing and diffusion of particles in the fluid.

The relationship between the concentration of motile microorganisms and L1 is depicted in Figure 13. As the L1 value increases, there is a decrease in the concentration of gyrotactic microorganisms. The density of microorganisms concerning the L2 is presented in Figure 14. As L2 increases, the concentration distribution of microorganisms decreases. This is attributed to the fact that a larger L2 signifies a lower Brownian motion diffusion coefficient, resulting in swimming microorganisms having a shallower penetration depth. Consequently, the distribution of microorganisms experiences a reduction with increasing L2. Figs. [15-17] represents the validity of inversion algorithms for concentration, temperature, and velocity profiles.

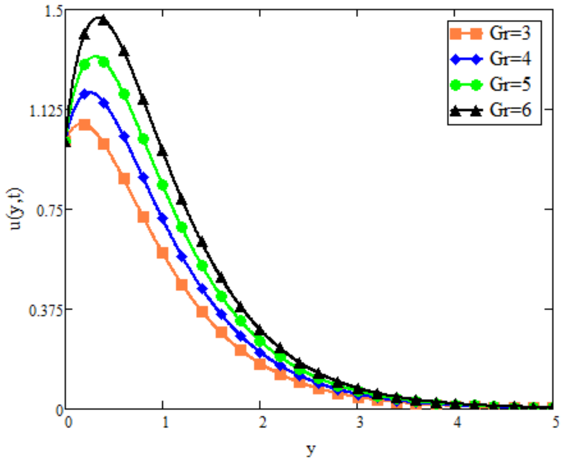

Figure 1: Velocity Profile u(y,t) for Parameter Gr

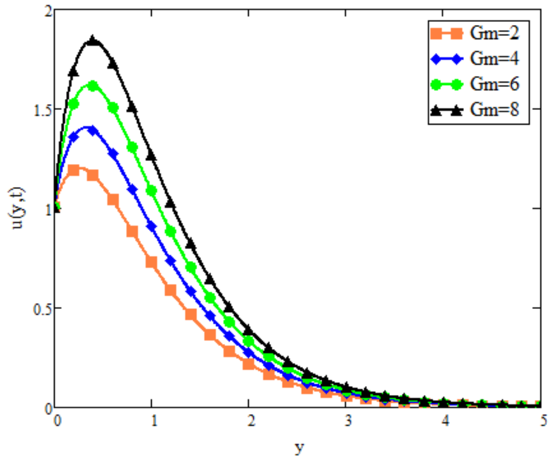

Figure 2: Velocity Profile u(y,t) for Parameter Gm

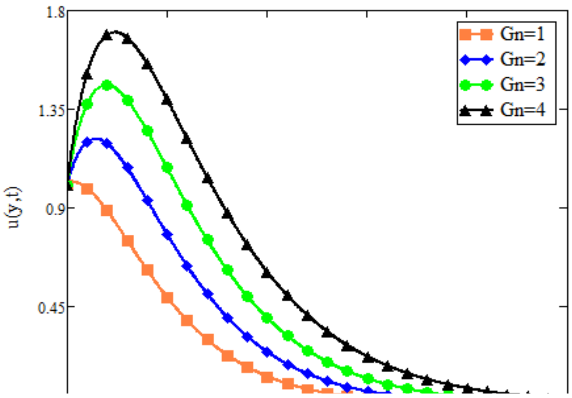

Figure 3: Velocity Profile u(y,t) for Parameter Gn

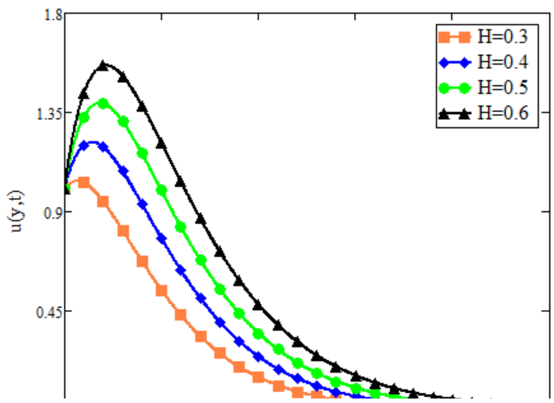

Figure 4: Velocity Profile u(y,t) for Parameter H

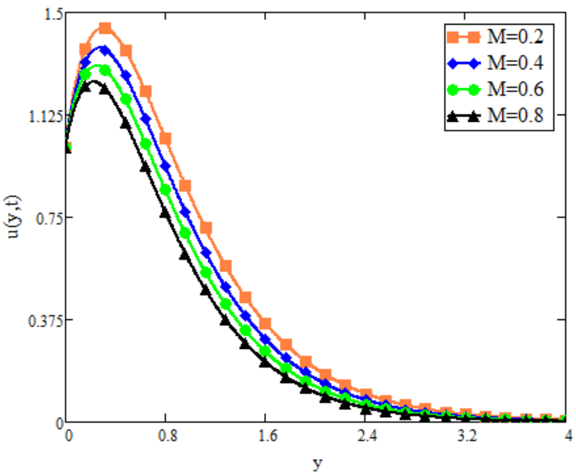

Figure 5: Velocity Profile u(y,t) for Parameter γ

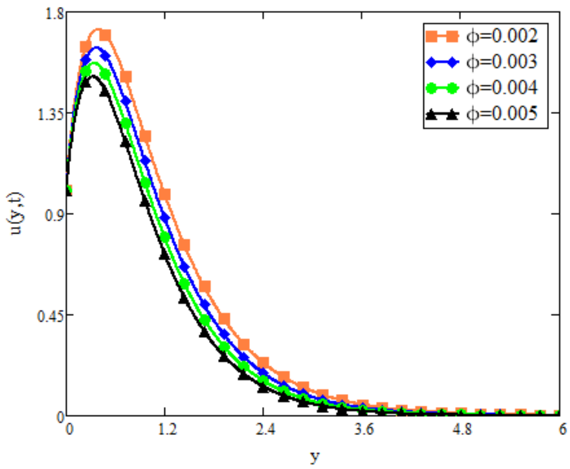

Figure 6: Velocity Profile u(y,t) for Parameter ϕ

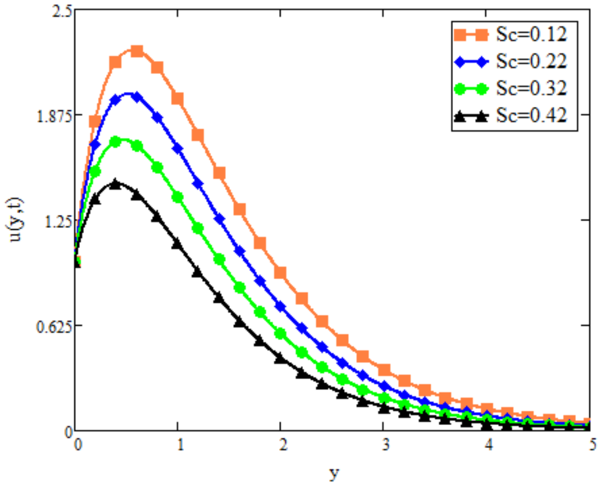

Figure 7: Velocity Profile u(y,t) for Parameter Sc

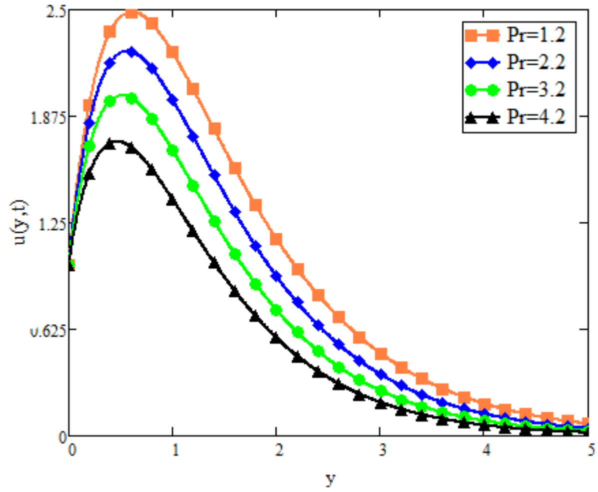

Figure 8: Velocity Profile v(y,t) for Parameter Pr

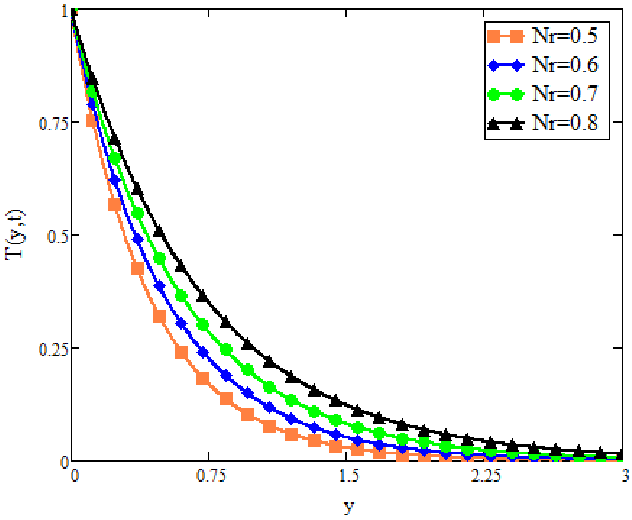

Figure 9: Temperature Profile T(y,t) for Parameter Nr

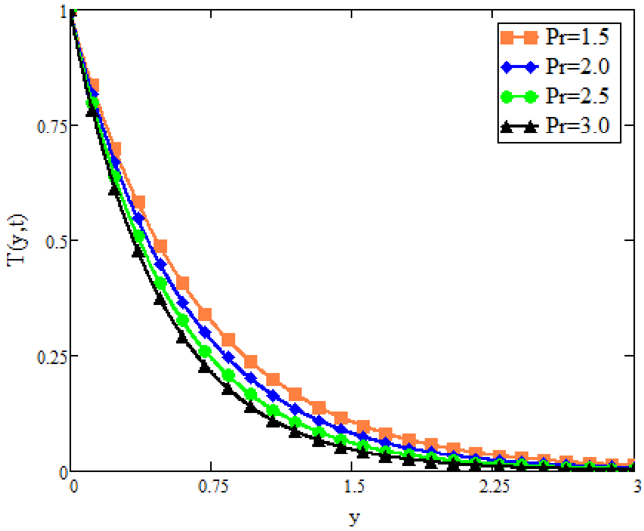

Figure 10: Temperature profile T(y,t) for Parameter Pr

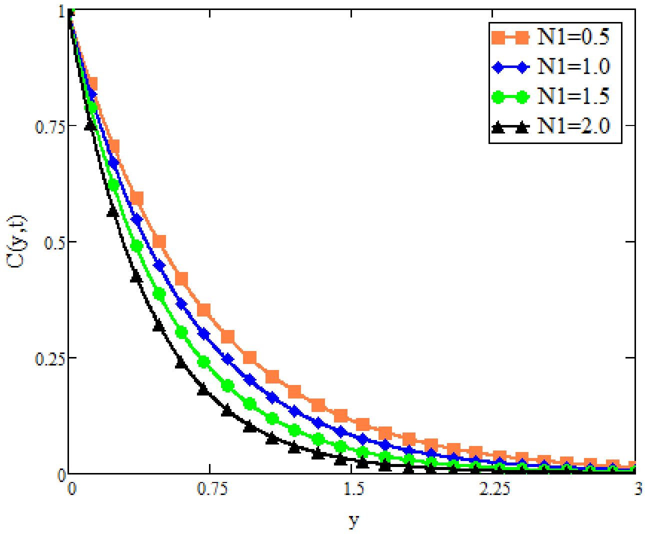

Figure 11: Concentration Profile C(y,t) for Parameter N1

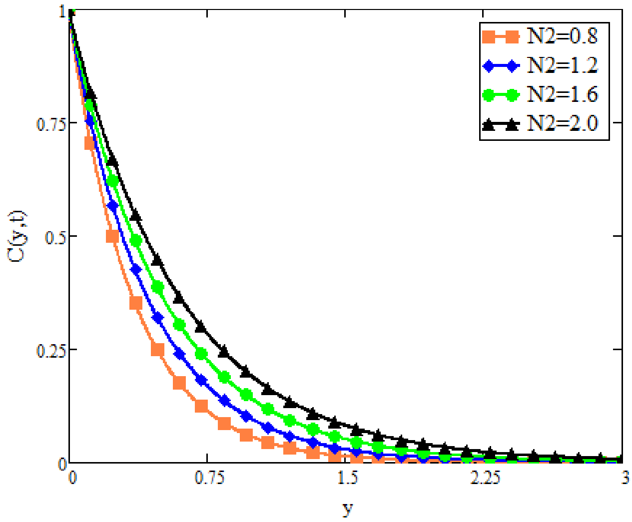

Figure 12: Concentration Profile C(y,t) for Parameter N2

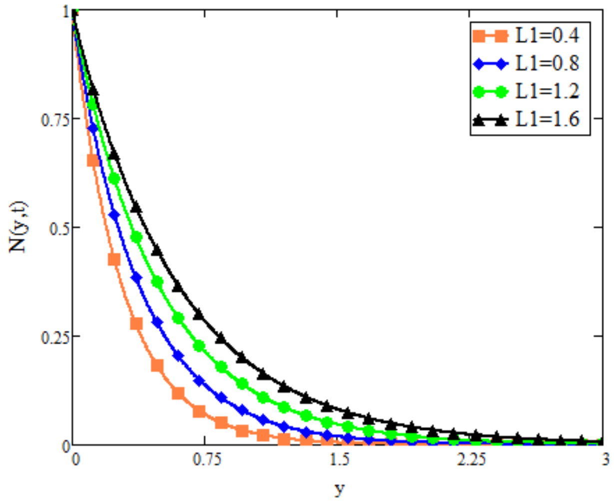

Figure 13: Bioconcentration Profile N(y,t) for Parameter L1

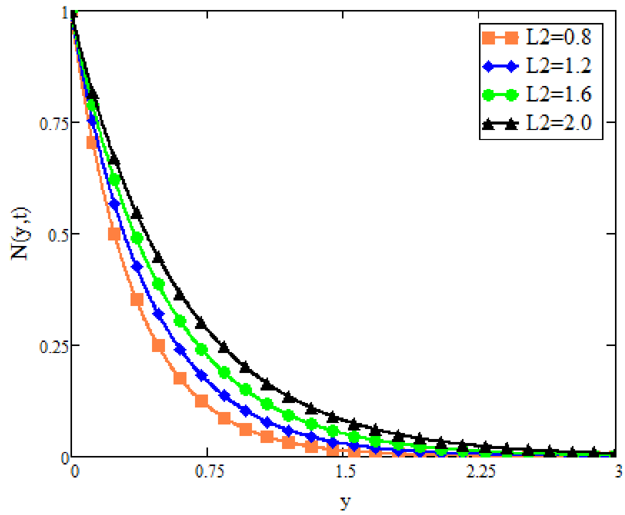

Figure 14: Bioconcentration Profile N(y,t) for Parameter L2

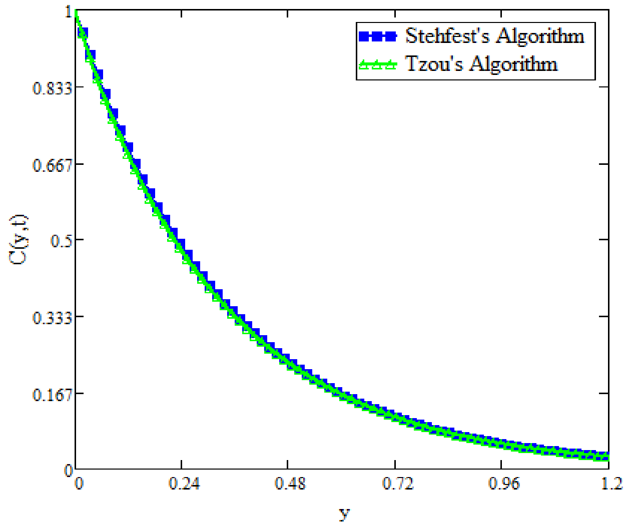

Figure 15: Concentration Profile C(y,t) Obtained by [39,40]

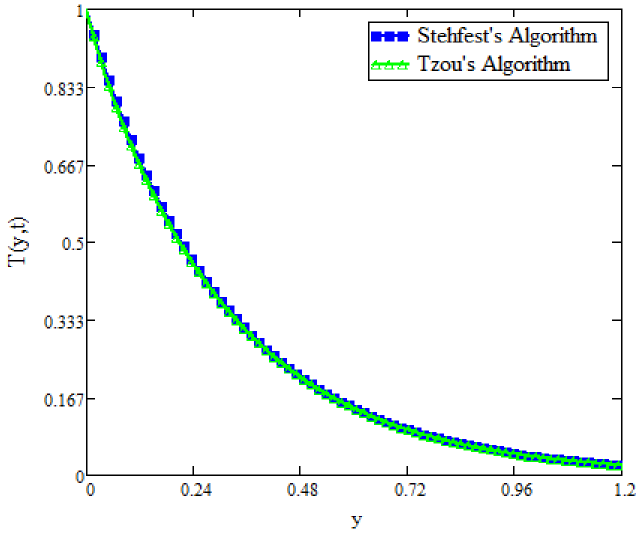

Figure 16: Temperature Profile T(y,t) Obtained by [39,40]

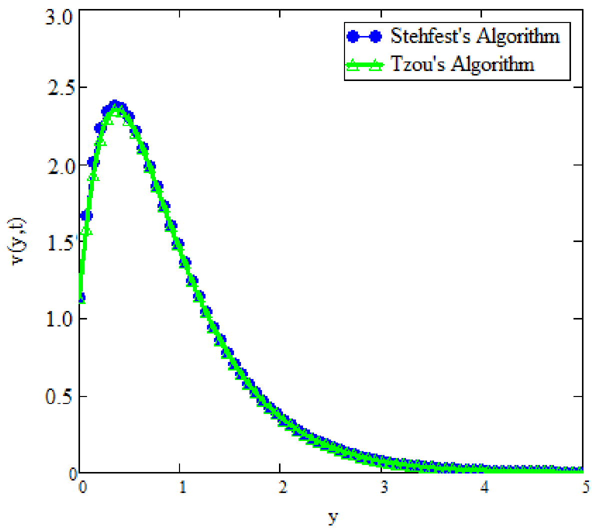

Figure 17: Velocity Profile C(y,t) Obtained by [39,40]

Citation: *Shafique, A., Ramzan, M., Nazar, M. (2024). Exploring the Role of Fractional Derivatives on Bioconvection Flow of Casson Fluids in the Solar System. Journal of Earth & Environmental Waste Management. 2(3), 1-13.*

3. Conclusion

This research delves into the dynamics of a Casson nanofluid subjected to electromagnetic hydrodynamics (EMHD) as it flows over a vertical plate. The study takes into account various factors such as solar radiation, gyrotactic microorganisms, and copper nanoparticles within a polyvinyl alcohol water-based fluid. Additionally, the analysis encompasses the effects of source terms like heat generation, thermal radiation, and chemical reactions.

To simplify the governing equations of fluid flow and boundary conditions, dimensionless variables are employed for nondimensionalization. Subsequently, the partial differential equations are transformed into ordinary differential equations, which are solved utilizing the constant proportional Caputo fractional derivative. The key findings of this study can be summarized as follows:

- An increase in fluid velocity is observed with higher values of Gr, Gm, E, γ, and Nr, while it decreases with increasing values of Gn, M, ϕ, and λ.
- Temperature profiles exhibit an increase with Nr, a, and ϕ, but decrease with higher values of Pr and Q.
- Mass concentration profiles show an increase with Nt, a, and ϕ, but decrease with higher values of Le, Kr, and N1.
- The bioconvection concentration profile increases with γ and ϕ but decreases with higher values of Lb and Pe.

One potential application of the analysis of Caputo fractional derivative on bioconvection flow of nanofluid with the application of solar energy is in the development of solar-powered nanofluid heat exchangers for water desalination. Water desalination is the process of removing salt from seawater to produce fresh water. It is a critical technology in many parts of the world where freshwater resources are scarce. Solar-powered nanofluid heat exchangers could be used to heat seawater to a temperature where the salt precipitates out, leaving behind fresh water. The Caputo fractional derivative analysis could be used to design these heat exchangers in a way that maximizes the efficiency of the desalination process.

References

1. Ramzan, M., Un Nisa, Z., Ahmad, M., & Nazar, M. (2021). Flow of Brinkman fluid with heat generation and chemical reaction. Complexity, 2021(1), 5757991.
2. VeeraKrishna, M., & Reddy, G. S. (2019). Unsteady MHD reactive flow of second grade fluid through porous medium in a rotating parallel plate channel. The Journal of Analysis, 27, 103-120.
3. Nazar, M., Fetecau, C., & Awan, A. U. (2010). A note on the unsteady flow of a generalized second-grade fluid through a circular cylinder subject to a time dependent shear stress. Nonlinear Analysis: Real World Applications, 11(4), 2207-2214.
4. Haq, S. U., ur Rahman, A., Khan, I., Ali, F., & Shah, S. I. A. (2018). The impact of side walls on the MHD flow of a second-grade fluid through a porous medium. Neural Computing and Applications, 30, 1103-1109.
5. Sheikh, N. A., Ali, F., Khan, I., & Saqib, M. (2018). A modern approach of Caputo–Fabrizio time-fractional derivative to MHD free convection flow of generalized second-grade fluid in a porous medium. Neural Computing and Applications, 30, 1865-1875.
6. Kataria, H. R., & Patel, H. R. (2018). Effect of thermo-diffusion and parabolic motion on MHD Second grade fluid flow with ramped wall temperature and ramped surface concentration. Alexandria Engineering Journal, 57(1), 73-85.
7. Shah, N. A., Areshi, M., Chung, J. D., & Nonlaopon, K. (2021). The New Semianalytical Technique for the Solution of Fractional-Order Navier-Stokes Equation. Journal of function spaces, 2021(1), 5588601.
8. Sene, N. (2022). Fractional model and exact solutions of convection flow of an incompressible viscous fluid under the Newtonian heating and mass diffusion. Journal of Mathematics, 2022(1), 8785197.
9. A. Razzaque, A. Rani, M. Nazar, Generalization of thermal and mass fluxes for the flow of differential type fluid with Caputo-Fabrizio approach of fractional derivative, Complexity, (2021), 1-11.
10. Chu, Y. M., Ikram, M. D., Asjad, M. I., Ahmadian, A., & Ghaemi, F. (2021). Influence of hybrid nanofluids and heat generation on coupled heat and mass transfer flow of a viscous fluid with novel fractional derivative. Journal of Thermal Analysis and Calorimetry, 144, 2057-2077.
11. Acharya, N. (2020). On the flow patterns and thermal behaviour of hybrid nanofluid flow inside a microchannel in presence of radiative solar energy. Journal of Thermal Analysis and Calorimetry, 141(4), 1425-1442.
12. Song, Y. Q., Obideyi, B. D., Shah, N. A., Animasaun, I. L., Mahrous, Y. M., & Chung, J. D. (2021). Significance of haphazard motion and thermal migration of alumina and copper nanoparticles across the dynamics of water and ethylene glycol on a convectively heated surface. Case Studies in Thermal Engineering, 26, 101050.
13. Jamshed, W., Eid, M. R., Safdar, R., Pasha, A. A., Mohamed Isa, S. S. P., Adil, M., ... & Weera, W. (2022). RETRACTED ARTICLE: Solar energy optimization in solar-HVAC using Sutterby hybrid nanofluid with Smoluchowski temperature conditions: a solar thermal application. Scientific reports, 12(1), 11484.
14. Sharma, B. K., Poonam, & Chamkha, A. J. (2022). Effects of heat transfer, body acceleration and hybrid nanoparticles (Au–Al2O3) on MHD blood flow through a curved artery with stenosis and aneurysm using hematocrit-dependent viscosity. Waves in Random and Complex Media, 1-31.
15. Nisa, Z. U., Shafique, A., Nazar, M., Asjad, M. I., Mahmoud, K. H., Alsubai, A. S., & Inc, M. (2022). A novel fractional study on free convection flow of Brinkmann hybrid nanofluid over an inclined plate. Thermal Science, 26(Spec. issue 1), 229-237.
16. Ramzan, M., Shafique, A., Rasid, M., Nazar, M., & Nisa, Z. U. (2022). Slippage flow of maxwell fluid over an inclined vertical plate with generalized heat and mass transfer. Journal of Advanced Research in Fluid Mechanics and Thermal Sciences, 99(2), 155-167.
17. Shafique, A., Ramzan, M., Ikram, Z., Amir, M., & Nazar, M. (2023). Mhd flow of jeffrey fluid with heat absorption and thermo-diffusion. Frontiers in Heat and Mass

Transfer (FHMT), 20(4), 1-10.
18. Shahzad, F., Jamshed, W., Eid, M. R., Safdar, R., Putri Mohamed Isa, S. S., et al. (2022). Thermal cooling efficacy of a solar water pump using Oldroyd-B (aluminum alloy-titanium alloy/engine oil) hybrid nanofluid by applying new version for the model of Buongiorno. Scientific Reports, 12(1), 19817.
19. Chaudhary, R. C., & Sharma, B. K. (2006). Combined heat and mass transfer by laminar mixed convection flow from a vertical surface with induced magnetic field. Journal of Applied Physics, 99(3).
20. Wang, Y. Q., Shafique, A., Nisa, Z. U., Asjad, M. I., Nazar, M., et al. (2022). Unsteady flow of Casson nanofluid through generalized Fourier's and Fick's law for heat and mass transfer. Thermal Science, 26(Spec. issue 1), 29-38.
21. Bresme, F., & Oettel, M. (2007). Nanoparticles at fluid interfaces. Journal of Physics: Condensed Matter, 19(41), 413101.
22. Zokri, S. M., Arifin, N. S., Kasim, A. R. M., & Salleh, M. Z. (2020). Flow of jeffrey fluid over a horizontal circular cylinder with suspended nanoparticles and viscous dissipation effect: Buongiorno model. CFD letters, 12(11), 1-13.
23. Sharma, M., Sharma, B. K., Gaur, R. K., & Tripathi, B. (2019). Soret and Dufour effects in biomagnetic fluid of blood flow through a tapered porous stenosed artery. Journal of Nanofluids, 8(2), 327-336.
24. Kumaraswamy Naidu, K., Harish Babu, D., Harinath Reddy, S., & Satya Narayana, P. V. (2021). Radiation and partial slip effects on magnetohydrodynamic Jeffrey nanofluid containing gyrotactic microorganisms over a stretching surface. Journal of Thermal Science and Engineering Applications, 13(3), 031011.
25. Shahzad, F., Jamshed, W., Nisar, K. S., Khashan, M. M., & Abdel-Aty, A. H. (2021). Computational analysis of Ohmic and viscous dissipation effects on MHD heat transfer flow of Cu-PVA Jeffrey nanofluid through a stretchable surface. Case Studies in Thermal Engineering, 26, 101148.
26. Giri, S. S., Das, K., & Kundu, P. K. (2019). Inclined magnetic field effects on unsteady nanofluid flow and heat transfer in a finite thin film with non-uniform heat source/sink. Multidiscipline Modeling in Materials and Structures, 15(1), 265-282.
27. Hassan, M., Faisal, A., & Bhatti, M. M. (2018). Interaction of aluminum oxide nanoparticles with flow of polyvinyl alcohol solutions base nanofluids over a wedge. Applied Nanoscience, 8, 53-60.
28. Choi, S. U., & Eastman, J. A. (1995). Enhancing thermal conductivity of fluids with nanoparticles (No. ANL/MSD/CP-84938; CONF-951135-29). Argonne National Lab.(ANL), Argonne, IL (United States).
29. Jang, S. P., & Choi, S. U. (2004). Role of Brownian motion in the enhanced thermal conductivity of nanofluids. Applied physics letters, 84(21), 4316-4318.
30. Bhattacharya, P. S. S. K., Saha, S. K., Yadav, A., Phelan, P. E., & Prasher, R. S. (2004). Brownian dynamics simulation to determine the effective thermal conductivity of nanofluids. Journal of Applied Physics, 95(11), 6492-6494.
31. Shafique, A., Nisa, Z. U., Asjad, M. I., Nazar, M., & Jarad, F. (2022). Effect of diffusion-thermo on MHD flow of a Jeffrey fluid past an exponentially accelerated vertical plate with chemical reaction and heat generation. Mathematical Problems in Engineering, 2022(1), 6279498.
32. Shukla, R. K., & Dhir, V. K. (2008). Effect of Brownian motion on thermal conductivity of nanofluids.
33. Baleanu, D., Fernandez, A., & Akgül, A. (2020). On a fractional operator combining proportional and classical differintegrals. Mathematics, 8(3), 360.
34. Asjad, M. I., Ikram, M. D., Ali, R., Baleanu, D., & Alshomrani, A. S. (2020). New analytical solutions of heat transfer flow of clay-water base nanoparticles with the application of novel hybrid fractional derivative. Thermal Science, 24(Suppl. 1), 343-350.
35. Saqib, M., Shafie, S., Khan, I., Chu, Y. M., & Nisar, K. S. (2020). Symmetric MHD channel flow of nonlocal fractional model of BTF containing hybrid nanoparticles. Symmetry, 12(4), 663.
36. Ali, R., Akgül, A., & Asjad, M. I. (2020). Power law memory of natural convection flow of hybrid nanofluids with constant proportional Caputo fractional derivative due to pressure gradient. Pramana, 94(1), 131.
37. Asjad, M. I., Ur Rehman, S., Ahmadian, A., Salahshour, S., & Salimi, M. (2021). First solution of fractional bioconvection with power law kernel for a vertical surface. Mathematics, 9(12), 1366.
38. Hassanzadeh, H., & Pooladi-Darvish, M. (2007). Comparison of different numerical Laplace inversion methods for engineering applications. Applied mathematics and computation, 189(2), 1966-1981.
39. Tzou, D. Y. (2014). Macro-to microscale heat transfer: the lagging behavior. John Wiley & Sons.
40. Stehfest, H. (1970). Algorithm 368: Numerical inversion of Laplace transforms [D5]. Communications of the ACM, 13(1), 47-49.